Astron. Astrophys. 323, 923–930 (1997)

ASTRONOMY
AND
ASTROPHYSICS

Magnetic reconnection in a magnetosphere-accretion-disk system

Axisymmetric stationary states and two-dimensional reconnection simulations

L. Rastätter[1] **and Thomas Neukirch**[2]

[1] Theoretische Physik IV, Ruhr-Universität, D-44780 Bochum, Germany
[2] School of Mathematical and Computational Sciences, University of St Andrews, Fife KY16 9SS, Scotland, UK

Received 23 October 1996 / Accepted 24 January 1997

Abstract. In the present paper we investigate the transport of accreting plasma across the magnetopause onto a strongly magnetized massive star (i.e. white dwarf or neutron star) by magnetic reconnection. A simplified axisymmetric magnetic field model of an aligned rotator is used to study the reconnection process. To be able to separate effects caused by instabilities of the system from intrinsic time-dependent behaviour, we first construct self-consistent stationary states of the magnetosphere-disk system. We include a rigid magnetospheric rotation and Keplerian rotation of the magnetized disk plasma.

The stationary states are computed numerically with a relaxation method which conserves the magnetic topology. Therefore we can prescribe an initial condition of the relaxation process using a magnetic field consisting of a dipole of the compact object and a homogeneous field threading the disk. The magnetopause then separates the regions of closed field lines with corotating plasma from open field lines with plasma in Keplerian motion.

The resistive stability of the stationary states is examined by two-dimensional magnetohydrodynamic simulations. We find that magnetic reconnection leads to mass transport across the magnetopause onto closed magnetic field lines The accretion disk material is accelerated along the magnetic field lines that are connected to the magnetic poles of the compact object and will eventually be accreted by the star at its polar caps.

Key words: accretion disks – neutron stars – white dwarfs – magnetohydrodynamics

1. Introduction

Magnetic fields are discussed to be important in the process of mass accretion onto massive objects. Strong magnetic fields are responsible for the focussing of accreted matter around the magnetic poles of the compact object leading to regularly pulsating intense high energy radiation of e.g. X-ray pulsars (see e.g. Frank et al.1985; Ventura & Pines 1991 and references therein). Furthermore variations of the luminosity observed over several rotation periods may also be explained by a strong magnetic field modifying the accretion process.

The modifications of the accretion process may be explained by various physical mechanisms. One possibility is a direct magnetic connection between the rigidly rotating compact object and the differentially rotating accretion disk as discussed by Ghosh & Lamb (1979). A steady state, however, will only be possible if the diffusion within the disk is strong enough to stop the winding-up of field lines in the differentially rotating plasma.

If the diffusion time-scale in the disk is larger than the difference in the rotation speeds of the accretion disk and the compact object magnetic energy will be built up due to the shear of field lines with formation of field-aligned currents. This energy is subsequently released by magnetic reconnection.

Flaring scenarios like this or other ones where the magnetic field is nearly excluded from the accretion disk have been considered by e.g. Aly (1980), Aly & Kuijpers (1990) and Van Ballegooijen (1994). Recently, time-dependent two-dimensional magnetohydrodynamic (MHD) simulations address the reconnection of twisted magnetic fields at magnetically threaded accretion disks (e.g. Matsumoto et al. 1996, Hayashi et al. 1996).

Another possibility is to explain the luminosity variations by a time-dependence of the accretion process itself. This possibility is especially attractive for magnetized objects because, as the experience with other magnetized objects like planets shows, a boundary layer forms between the plasma inside the magnetosphere and the matter outside. The latter can only penetrate into the magnetosphere across the magnetopause if the constraint of ideal MHD is violated at least locally and a magnetic connection between the magnetospheric and the accretion disk field is established. This process of magnetic reconnection across the magnetopause is intrinsically time-dependent as theory and observations of plasma transport at planetary (e.g. the Earth's) magnetopauses show (see e.g. Elphic 1990; Lockwood 1991; Nishida 1989; Otto & Birk 1992; Paschmann et al. 1982; Shi et al. 1991). Thus magnetic reconnection naturally explains time variability of accretion and of the corresponding radiation.

Send offprint requests to: L. Rastätter

Instabilities of the magnetopause of compact objects as the Kelvin-Helmholtz instability have been discussed before (e.g. Anzer & Börner 1979, 1980; Wang & Robertson 1984). Under ideal conditions, however, these instabilities cannot allow for transport of plasma across the magnetopause but they may facilitate the onset of reconnection.

In the present paper we investigate the resistive transport across the magnetopause between the magnetosphere of a compact object and its accretion disk. Since we want to study the instability it is important to exclude any time-dependent phenomena which are not due to instability. So we want to start our non-ideal evolution from an ideally stable stationary state of the magnetosphere-disk system. A steady state of this system is only possible under the simplifying assumption of axisymmetry which also facilitates the numerical treatment. This assumption may be regarded as a compromise between the requirements of a realistic model and numerical feasibility.

We have two major objectives in this paper: a) the construction of self-consistent axisymmetric stationary states of the magnetosphere-disk system and b) the investigation of the resistive instabilities of this system.

The calculation of stationary states of rotating accreting systems is inherently difficult. Analytical approaches have only been carried out under simplifying assumptions of vanishing rotation (e.g. Uchida & Low 1981) or have included an infinitely thin accretion disk as a discontinuity of a large-scale magnetic field (e.g. Aly 1980). These models are not suitable for our analysis. We want to model a rigidly rotating magnetosphere and an accretion disk of finite thickness rotating nearly at Keplerian speed. These two regions are separated by a magnetopause. Since the shape of the magnetopause cannot be prescribed *a priori*, we have a free-boundary problem which is solved numerically by a relaxation method. To the best of our knowledge, our solutions are the first self-consistent axisymmetric stationary states ever found for a rotating magnetosphere-disk system. The relaxation method we have used has been successfully applied to other problems (Hesse & Birn 1993; Rastätter et al. 1994). The relaxation uses a magnetic field configuration representing a magnetic dipole field of the compact object which is aligned with its rotation axis and a homogeneous field representing the advected field in the disk. The magnetic topology is conserved during the relaxation process which fully ensures the validity of Ferraro's law of isorotation in contrast to our earlier treatment of this problem (Rastätter & Schindler 1996). The relaxation method is described in Sect. 2 and the results are described in Sect. 4.

The stationary states are then used as initial conditions for the resistive time-dependent evolution. This investigation is carried out with two-dimensional axisymmetric resistive MHD simulations. By introducing a localized patch of resistivity at the magnetopause we initiate resistive instability leading to magnetic reconnection and plasma transport across the magnetopause. The code used has been successfully applied to numerous space and astrophysical problems (Birn 1980; Otto 1990; Birn & Hesse 1991; Birk & Otto 1996; Dreher et al. 1996; Fleischer & Schindler 1996; Hesse & Birn 1993). This way of modeling resistive instability is motivated by observational and theoretical studies of planetary magnetospheres (e.g Haerendel et al. 1978; Elphic 1990; Otto & Birk 1992, 1993).

The resulting time-dependent evolution is described in Sect. 4 and the paper is concluded with a summary and discussion of the main results in Sect. 5.

The following resistive reconnection phase shows how reconnection accelerates the disk matter and allows its penetration into the magnetosphere which is inhibited in ideal MHD by the frozen-in condition. In contrast to reconnection computations by Hayashi et al. (1996) we start from an equilibrium state without stellar field lines threading the Keplerian rotating disk.

2. Numerical relaxation method

In the relaxation stage a method is employed which already has been successfully used (Hesse & Birn 1993; Rastätter et al. 1994) to compute equilibria in the framework of IMHD. The set of equations used in the relaxation stage are the IMHD equation in the poloidal plane (r, z) in cylindrical coordinates modified by terms arising from the relaxation method. Plasma velocity components which are zero in equilibrium are damped to approach equilibrium during the relaxation procedure:

$$\frac{\partial \rho}{\partial t} = -\nabla(\rho \boldsymbol{v}_p) \tag{1}$$

$$\frac{\partial \boldsymbol{v}_p}{\partial t} = \frac{-\nabla p + \boldsymbol{j}_t \times \boldsymbol{b}_p}{\rho_a} + \frac{\rho}{\rho_a}\left(\frac{v_t^2}{r}\frac{\boldsymbol{r}}{r} + \boldsymbol{g}\right) - \frac{\boldsymbol{v}_p}{\tau_D} \tag{2}$$

$$v_t = \Omega r \tag{3}$$

$$\frac{\partial \boldsymbol{b}_p}{\partial t} = \nabla\times(\boldsymbol{v}_p \times \boldsymbol{b}_p) \tag{4}$$

$$(\boldsymbol{b}_p \cdot \nabla)\Omega = 0 \tag{5}$$

$$\nabla\cdot\boldsymbol{b} = 0 \tag{6}$$

$$\boldsymbol{j}_t = \nabla\times\boldsymbol{b}_p \tag{7}$$

$$\frac{\partial p}{\partial t} = -\nabla\cdot(p\boldsymbol{v}_p) - (\gamma-1)p\nabla\cdot\boldsymbol{v}_p \tag{8}$$

$$\boldsymbol{g} = -\nabla\left(\frac{m}{\sqrt{r^2+z^2}}\right) \tag{9}$$

$$\rho_a = 1. \tag{10}$$

Here ρ denotes the mass density, m the mass of the star (multiplied by the gravitational constant), t time in Alfvén times, $\boldsymbol{b}$ the magnetic field, $\boldsymbol{v}$ plasma flow velocity, p plasma pressure, $\boldsymbol{j}$ current density and γ the ratio of specific heats. The quantity ρ_a is an artificial density used for rapid pseudo-dynamic relaxation by the damping term $-\boldsymbol{v}_p/\tau_D$ in Eq. (2). The parameters $\tau_D, \tau_{D,T}$ in Eqs. (2) and (3) in the relaxation terms may be chosen independently to obtain fast relaxation. Furthermore we use $\gamma = 5/3$ for adiabatic dynamics during relaxation. In the reconnection phase the latter choice is still justified together with the neglect of heat transport and radiation effects as we consider only short time scales compared to radiative and diffusive time.

The equations used are written in dimensionless form indicated by lowercase symbols. The magnetic field is normalized to the homogeneous background field B_0 oriented in z-direction,

ρ to a typical magnetospheric value, p to $B_0^2/4\pi$, length scales to the radius R_N of the compact object, velocities to the magnetospheric Alfvén velocity $V_A = B_0/\sqrt{4\pi\rho_0}$ and time scales to the Alfvén time scale $\tau_A = R_N/V_A$. The normalization of the velocities also gives the normalized values of the product of the gravitational constant and the mass of the central object (here denoted by m).

The index p indicates that the equations refer to the poloidal components of the magnetic field $\boldsymbol{b}$ and plasma velocity $\boldsymbol{v}$ while index t refers to the component in toroidal (invariant) direction φ. The current density is purely toroidal in the relaxation phase from Eq. (8) as $b_\varphi = 0$ and because of the two-dimensionality $\partial/\partial\varphi = 0$. The term $(\boldsymbol{v}_t^2/r)\boldsymbol{r}/r$ in Eq. (2) is the centrifugal force appearing in cylindrical coordinates. The velocity $v_\varphi = v_t$ is computed from the angular velocity Ω in Eq. (3). Eq. (5) insures that b_φ remains zero all the time. So the integration of b_φ is not needed at the relaxation stage and Eq. (4) is sufficient as induction equation.

Depending on the location of the magnetospheric boundary (magnetopause), Ω is prescribed on the boundary ($z = 0$). The magnetopause is convected with the poloidal fluid velocity making use of the fact that the plasma is 'frozen' in the magnetic field in ideal MHD.

In Eq. (2) an additional term $(-\rho\boldsymbol{v}/\tau_D)$ is added to make the dynamic system relax into a new equilibrium (Hesse & Birn 1993; Rastätter et al. 1994).

The relaxation method has been refined compared to the previous work (Rastätter & Schindler 1996), giving suitable starting configurations for the study of resistive dynamics which consistently incorporate Ferraro's law of isorotation. Additionally, some of the input parameters have been changed so that the different time scales are of comparable order of magnitude:

These main time scales in a magnetosphere accretion disk system are associated (reciprocally) to the fundamental velocities in the system:

Alfvén velocity: The fastest velocity in numerical simulations is the Alfvén speed V_A defined by $V_A = \sqrt{b/\rho}$ in the magnetosphere where the magnetic field is strong and the mass density small. As the fastest velocity the Alfvén velocity limits the time step δt which can be used by an explicit integration scheme used in our approach with spatial resolution δx by the well-known Courant-Friedrich-Levy (CFL) condition $\delta t < \delta x/V_A$.

Rotation velocity: The parameter representing the gravitation (central mass) was adjusted to get a toroidal rotation velocity $v_\varphi = \Omega r = \mathcal{O}(1)$ with $v_\varphi = \sqrt{GM/r_0}$ the Keplerian velocity V_K at a radius r_0 in the middle of the simulation box. The rotation of the magnetosphere is assumed to be slightly smaller then the Keplerian rotation ($0.8V_K$).

Sound velocity: The mass densities in the magnetosphere and the disk were chosen that the sound velocities are of order 1 in the magnetosphere and of order 10^{-2} in the accretion disk leading to a large radial scale height in the magnetosphere and a small scale height in z-direction in the disk.

The hierarchy of time scales connected with the velocities is almost realistic according to viscous accretion disk models (e.g. Pringle & Rees 1972, Shakura & Sunyaev 1973). However, the Alfvén speed of the magnetosphere is too small compared to the disk rotation velocity. This choice has to be made to obtain a numerically treatable set of time-scales associated with the mentioned basic velocities.

As only a small portion of the accretion disk is included, a disk equilibrium with constant temperature is assumed in contrast to more refined disk models. To reveal the basic properties of the plasma dynamics in a small region around the magnetopause this should be sufficient.

3. Setup and computation of equilibrium states

In this paper two magnetic field configurations are examined which are derived from a dipole embedded into a homogeneous field parallel to the polar axis (z-axis) without x-line in the equatorial plane (Fig. 1). This configuration has been used already in Rastätter & Schindler (1996). The field directions are sketched in Fig. 2. The poloidal flux-function in this case is

$$\psi = \frac{\mu r^2}{\left(r^2+z^2\right)^3} + \frac{B_{z0}}{2} r^2 \tag{11}$$

with $\mu = -5 \cdot 10^5$ and $B_{z0} = 1$ being the magnitudes of the magnetic moment of the star and of the external field, respectively, to give equal strength of both at the equatorial radius of the magnetosphere $r_0 = 100$ (in units of R_N). The computation box extends from $r = 90$ to $r = 110$ and from $z = 0$ to $z = 20$ (i.e. a meridional cut above the equatorial plane). We make use of the symmetry of the system at the equatorial plane at $z = 0$ taking only the upper part above the equatorial plane. The grid resolution is 0.1 in both directions (r,z) to resolve the whole current layer at the magnetopause two-dimensionally as its shape is *a priori* unknown and to be able to simulate the resistive dynamics there properly. The initial pressure and density distribution are the same as in Rastätter & Schindler 1996 (see Fig. 4) with a disk-magnetosphere ratio of the density $\rho_D/\rho_M = 40$ instead of 10^5 and the disk pressure being $P_D = 0.4$ instead of 1. The disk temperature T_D is equal to $P_D/\rho_D = 0.01$. The fastness parameter of the rotation speed of the central object $f = \Omega_*/\Omega_{Kepler}(r_0)$ is set to 0.8. R denotes the radial distance from the central object $R = \sqrt{r^2+z^2}$.

$$p_D = P_D \exp\left[\frac{GM}{kT_D}\left(\frac{1}{R}-\frac{1}{r}\right)\right] \tag{12}$$

$$p_M = P_M \exp\left[\frac{GMf^2}{kT_M r_0}\left(\frac{r^2}{r_0^2}-1\right) + \frac{GM}{kT_M}\left(\frac{1}{R}-\frac{1}{r}\right)\right] \tag{13}$$

The disk thickness z_0 remains the same (about 5 in Fig. 4) as the gravitation parameter is enhanced by 10^3 giving also a 30-fold larger toroidal rotation velocity ($v_\varphi \simeq 3$) as compared to Rastätter & Schindler (1996). The prescription of isorotation instead of z-independent rotation in the disk leads to a slight force imbalance above the disk which disappears during relaxation as

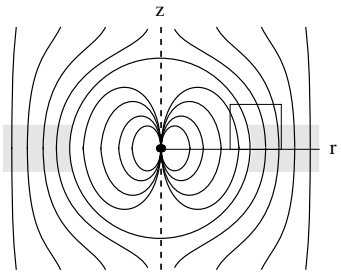

Fig. 1. Sketch of the initial rotational symmetric magnetosphere-disk model. The magnetosphere rotating rigidly with the central star is enclosed in a circle around the star in the middle. The accretion disk is roughly represented by the shaded region outside the magnetopause circle. The dipole axis (z-axis, dashed) is aligned with the direction of the angular velocity vector Ω. The two-dimensional computational domain is indicated by the rectangle above the equatorial plane (r-axis).

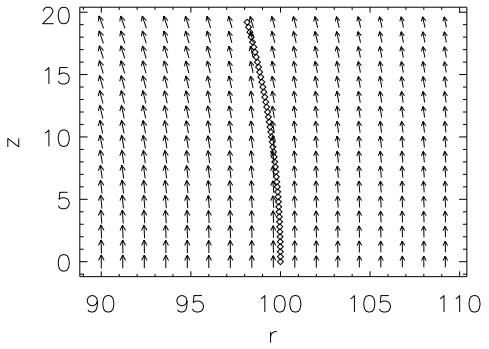

Fig. 2. The magnetic vector field in the non-reversal case ($b_{par.}$).

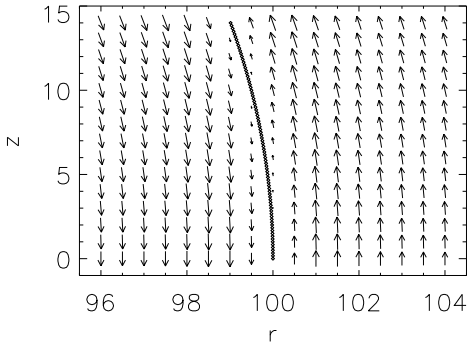

Fig. 3. The magnetic field lines in the reversal case ($b_{antipar.}$), shown in a smaller part of the domain of Fig. 1. The field direction is reversed in the magnetosphere and hence at the magnetopause the field is zero. Note that the distance between the arrows does not reflect the grid resolution which is much finer.

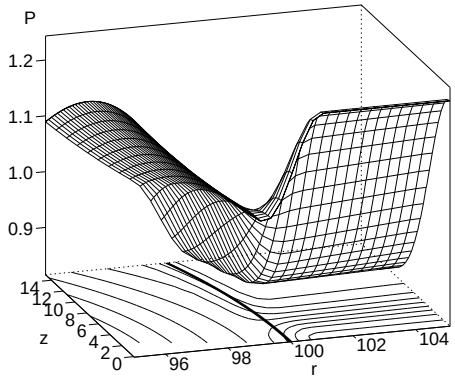

Fig. 4. The gas pressure p in the initial setup of Fig. 2. The accretion disk pressure with magnitude P_D = 0.4 (Eq. 12) in this case is added to an underlying background given by a constant disk coronal pressure of about 0.8. The magnetosphere pressure is given by the stratification of the gas in the gravitational field with rotation (Eq. 13).

well as the imbalance arising from the inner edge of the disk pressure distribution.

In the case of field reversal (Fig. 3) the resulting $\boldsymbol{j} \times \boldsymbol{b}$ force at the magnetopause has to be balanced by an extra pressure which is nearly given by adding the missing magnetic pressure $(b^2_{par.} - b^2_{antipar.})/2$ compared to the case without field reversal ($b_{par.}$, Fig. 2). More detailed derivations of the compensation were not made as the curvature effects (the $(\boldsymbol{b}\cdot\nabla)\boldsymbol{b}$-term) cannot be compensated by a scalar function anyway.

In Fig. 5 one can see the magnetic field in the second case after the relaxation phase. The magnetopause has moved inward with the plasma frozen into the field. Fig. 6 shows the equicontours of the angular velocity after relaxation. The transition region between the rigid rotation (left) and the Keplerian rotation (on the right) is determined by the Ω-prescription at $z = 0$. The contours exactly follow the direction of the magnetic field vectors (Fig. 5).

The force density has diminished by a factor of more than 100 to a level which will not decrease further due to discretization errors. The problem of numerical diffusion is outlined in the next section.

4. The resistive phase

4.1. Description of initial configuration and changes due to resistive MHD

The resistive phase is implemented in the following manner:

- The plasma velocity in the poloidal plane is set to zero while the toroidal component remains unchanged.
- The relaxation terms are switched off and the full nonlinear terms $(\boldsymbol{v} \cdot \nabla)\boldsymbol{v}$ are switched on as well as the evolution of b_φ.
- At the magnetopause a localized resistivity is imposed where reconnection can start.

The Eqs. (4) and (5) are replaced by the full induction equation

$$\frac{\partial \boldsymbol{b}}{\partial t} = \nabla\times(\boldsymbol{v}_p \times \boldsymbol{b}_p - \eta \boldsymbol{j}) \tag{14}$$

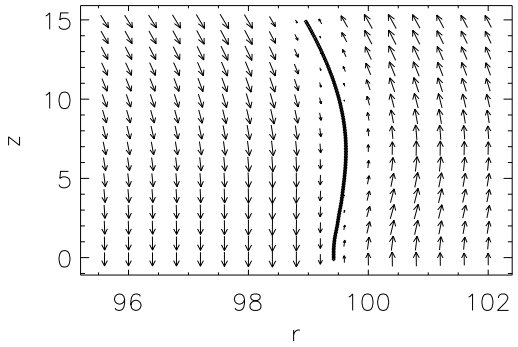

Fig. 5. The magnetic field 3 after relaxation with change of the shape of the magnetopause.

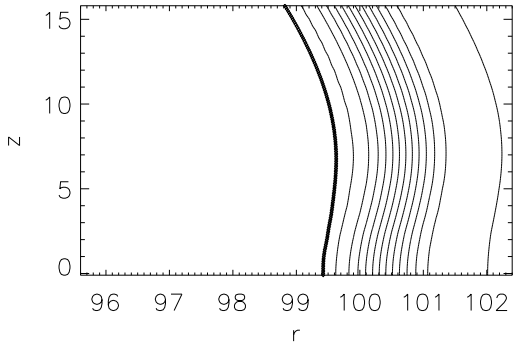

Fig. 6. The angular velocity Ω: The contour lines are parallel to the magnetic field orientation (Fig. 5).

and Eqs. (2, 3) become the full equation for all components of the plasma velocity.

$$\frac{\partial \boldsymbol{v}}{\partial t} = -(\boldsymbol{v}\cdot\nabla)\boldsymbol{v} + \frac{-\nabla p + \boldsymbol{j}\times\boldsymbol{b}}{\rho} + \boldsymbol{g}. \quad (15)$$

4.2. Results of resistive simulations

During the resistive phase the magnetopause location stays fixed and diagnostics reveals the mass and energy fluxes across this border.

Several different situations may be considered:

- magnetic field parallel or anti-parallel as described above
- different location of the reconnection site on the magnetopause (at $z = 0$ and $z = 4$).
- variation of the localized resistivity (between $\eta = 0.$ and $\eta = 0.1$)
- different disk pressure and mass density in the case without field reversal to obtain different current densities j_φ at the magnetopause.

In this paper the effect of the field line configuration (first item) is shown for a fixed resistivity at $z = 0$ with magnitude 0.01. The other changes have also been examined. The results do not show fundamentally different results. We may note that the range of resistivity is limited on both sides. Zero resistivity eventually leads to numerical diffusion or numerical reconnection (in the case of anti-parallel fields) due to the discretization on the rectangular grid. The curved boundary layer is not properly represented to maintain ideal stability from the numerical point of view. A small resistivity $< 10^{-4}$ is the lowest limit which can be distinguished form "ideality". For high values of η magnetic diffusion becomes dominant compared to reconnection. The current density decays faster than reconnection is able to enhance the current density at the site where $\eta \neq 0$. To see the difference between unstable (fast reconnecting) and stable cases a resistivity of medium magnitude (0.01) is chosen.

The first example is the anti-parallel field case which is expected to be highly unstable with respect to magnetic reconnection. Although the magnetic energy is only 10 % of the gravitational (rotational, kinetic) energy of the disk matter acceleration along the field lines to high latitudes is possible as the magnetic field lines roughly follow the equicontours of the gravitational potential (circles around the star at the origin). In this configuration disk matter can easily be accelerated to flow to the magnetic poles of the massive star to be accreted there. Due to the mass flow the inner edge of the disk retreats from the magnetosphere and new matter has to be accumulated there to trigger a new reconnection event.

However, if the field is not anti-parallel across the magnetopause, reconnection will not play any role unless a significant shear component b_φ is present. In this case the reconnection process operates more slowly and the flow pattern becomes more diffusion-like (Fig. 11) as seen from the mass density distribution (Fig. 12). Fig. 13 qualitatively shows the mass transfer into the magnetosphere during the resistive phase for the two magnetic field orientations investigated. At the end of the simulations the mass content of the magnetospheric part of the simulation domain has increased by at most 20 % from the initial value. In the case of fast reconnection the mass entering the magnetosphere grows exponentially (solid line). In the other case the mass diffuses steadily into the magnetosphere (dashed line).

5. Summary and discussion

In the present paper we have investigated the mass transport across the magnetopause between the magnetosphere and the accretion disk of a compact object in the framework of resistive magnetohydrodynamics. We have done this under the simplifying assumption of axisymmetry for two reasons: a) axisymmetry allows for construction of steady states with which the time-dependence due to resistive instability can be studied, independent from the time-evolution of non-axisymmetric states and b) it drastically reduces the numerical problems to be solved.

In the first step we presented a method how to construct the required stationary states. The rigidly rotating region of closed field lines (the magnetosphere) and a region of open field lines rotating at almost Keplerian velocity (the accretion disk) are separated by the current-carrying boundary-layer (the magnetopause) whose shape is computed self-consistently. This was

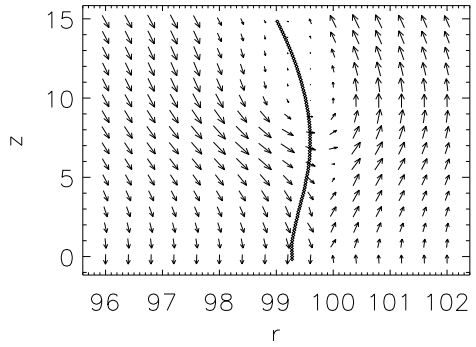

Fig. 7. The magnetic field with reconnection after $50\tau_A$. An X-point forms at the reconnection site located at the magnetopause on the equatorial plane where $\eta \neq 0$. During the reconnection process the X-point has moved slightly outward with the inner edge of the disk (seen in the mass density plot Fig. 10).

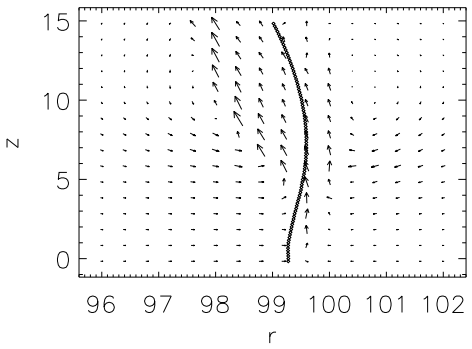

Fig. 8. Corresponding plasma velocity pattern. The disk plasma is accelerated to high poloidal velocities and enters the magnetosphere along the magnetic field lines.

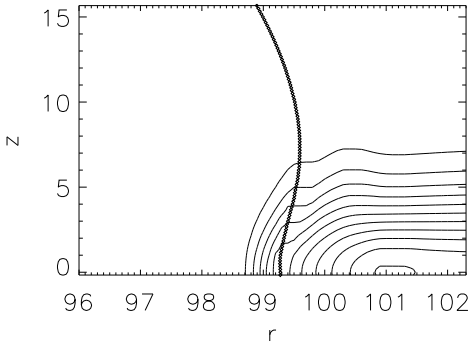

Fig. 9. Contour plot of the mass density at the onset of the reconnection phase. The mass density has a sharp gradient at the magnetopause where typical values are 1 (left side, magnetosphere) and 23 - 0.25 (right (disk) side, at z = 0 and z = 15 respectively)

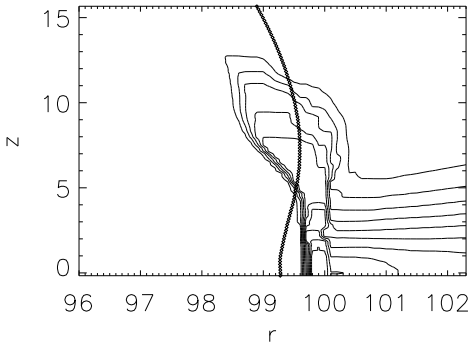

Fig. 10. Contour plot of the mass density during reconnection. The maximum values are in the disk (on the right of the magnetopause) at z = 0 ($\rho_{max} \simeq 20$). Substantial parts of the mass from the inner edge of the disk enter the magnetosphere and reach higher z-regions. The density range is the same as in Fig. 9.

achieved by prescribing the initial topology of the magnetic field (dipole and superposed homogeneous background field) and using a relaxation method preserving magnetic topology. The stationary states show the typical qualitative structure of analytical magnetosphere-accretion disk systems (e.g. Aly 1980, Aly & Kuijpers 1990, Ghosh & Lamb 1979). with a magnetosphere squeezed by the accretion disk at the equatorial plane. The law of isorotation which is necessary to obtain stationary states is also fully incorporated in the relaxation scheme. This is an important improvement compared to the works of Uchida & Low (1981) without rotation at all and of Rastätter & Schindler (1996) without the complete inclusion of isorotation.

In a second step we used a resistive MHD code to follow the time-evolution of the system with the stationary states as initial configurations. Introduction of a localized resistivity at the magnetopause leads to instability of the formerly stationary states and to magnetic reconnection. Subsequently plasma is transported from the accretion disk into the magnetosphere. This plasma flows along the magnetic field lines towards the polar caps of the compact object and though the caps are not included in our computational domain, we may speculate that the matter will eventually be accreted there by the compact object. This result is consistent with the scenario commonly discussed in the literature and thought to be responsible for the generation of pulsed high-energy radiation from compact objects (e.g. Aly & Kuijpers 1990; Frank et al. 1985; Ventura & Pines 1991).

We presented 2D simulations of an axisymmetric system starting from previously calculated stationary states and followed the evolution of an instability at the magnetopause whereas Hayashi et al. (1996) deal with a time-dependent system because the field lines threading the accretion disk do not obey Ferraro's isorotation law. In our model none of the field lines does initially connect the compact object with any part of the accretion disk. During the reconnection process such a connection is formed. It would be interesting to investigate the long-term behaviour of the resistive dynamics as more and more material enters the magnetosphere. In the case of parallel fields at the magnetosphere, we presented here, it may be possible that this material forms an inner edge of the accretion disk *inside* the magnetosphere. Processes observed by Hayashi et al. could well

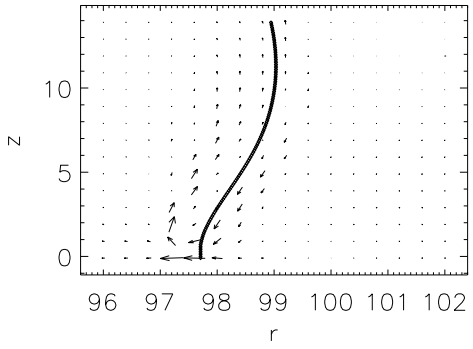

Fig. 11. The velocity pattern in the parallel field case is by a factor of 30 slower than in the highly unstable reconnection case of Fig. 8.

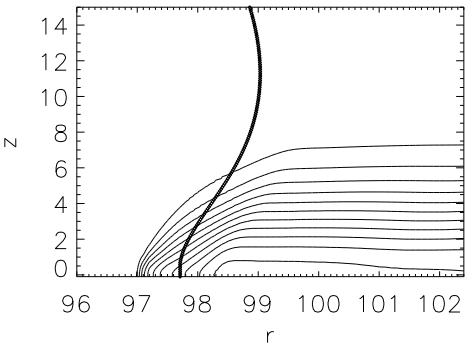

Fig. 12. Mass density in the parallel field case: No mass at high latitude can be seen in this case as in Fig. 10 due to the weaker flow which consists mainly of diffusion across the field lines at small z (Fig. 11).

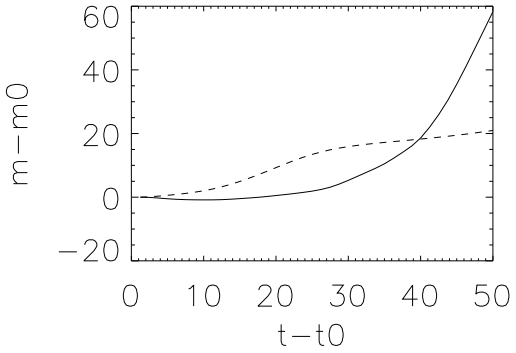

Fig. 13. Mass accumulation in the magnetosphere over $50\tau_A$ in the case of fast reconnection of Fig. 7 (solid line) and of slow reconnection of Fig. 2 (dashed line). The maximum values at the end of the simulation are about 10 to 20 % of the mass of the magnetosphere in the computation domain $m0$ at the onset time of reconnection $t0$. Note that the absolute values of the mass flux cannot be compared directly as some input parameters (e.g. accretion disk mass and pressure) are different.

be important there. This is beyond the numerical capabilities at the present time and will be a subject of further work.

There are several ways to generalize and improve the present model. First of all we have not included a toroidal magnetic shear field (b_φ) in the stationary states which effects the resistive evolution. Only the cases of parallel and anti-parallel magnetic field at the magnetopause have been considered in this paper. As the reconnection rate grows with the angle between the magnetic field lines outside of the magnetopause current layer of the magnetosphere-disk system (e.g. Otto 1990) we would expect that an arbitrary magnetic shear leads to reconnection even if the angle is not 180 degrees. In this sense the cases studied in this work are the most stable and unstable configurations possible.

Furthermore, general models of accretion disks propose a magnetic field that is neither symmetric nor laminar: The field is not smooth and consists of structures with typical dimensions which are smaller than the disk scale height as indicated by simulations of the highly turbulent fluid in the accretion disk leading to field generation inside the disk and a corona around the disk by dynamo action (see e.g. Torkelsson & Schramkowski 1996). These small magnetic loops may also reconnect with the magnetospheric field of the compact object (e.g. Aly & Kuijpers 1990; Kuijpers 1995) at the magnetopause. On top of that the assumption of axisymmetry cannot be kept in more realistic models as the observed variation of the emitted radiation is generally explained with an obliquity of the rotation axis with respect to the magnetic axis of the compact object (e.g. Pringle & Rees 1972; Aly & Kuijpers 1990; Frank et al. 1985; Ventura & Pines 1991). The resulting configurations will become much more complicated and no symmetry may be assumed for the initial state. In this case it is no longer possible to calculate stationary states like those presented here as the whole system is intrinsically time-dependent. These aspects of refined models are to be addressed in future three-dimensional simulations.

Acknowledgements. Part of this work was supported by the German *Deutsche Forschungsgemeinschaft, DFG* project number Schi 156-14/2 (LR). TN thanks PPARC for his support. The authors are also grateful for support by a British-German Academic Research Collaboration Grant.

References

Aly, J.J. 1980, A&A, 86, 192
Aly, J.J., Kuijpers, J. 1990, A&A, 227, 473
Anzer, U., Börner, G. 1979, ESA-SP 148, 8
Anzer, U., Börner, G. 1980, A&A, 83, 133
Birk, G.T., Otto, A. 1996, J. Comp. Phys., 125, 513
Birn, J. 1980, J. Geophys. Res., 85, 1214
Birn, J., Hesse, M. 1991, J. Geophys. Res., 96, 23
Dreher, J., Birk, G.T., Neukirch, T. 1997, A&A, in press
Elphic, R.C. 1990, in Physics of Magnetic Flux Ropes, Geophys. Monogr. 58, AGU, Washington D.C., p. 455
Fleischer, J., Schindler, K. 1996, Astrophys. Lett. & Comm., 34, 237
Frank, J., King, A.R., Raine, D.J. 1985, Accretion Power in Astrophysics, Cambridge Univ. Press
Ghosh, P., Lamb, F.K. 1979, ApJ, 232, 259
Hayashi, M.R., Shibata, K. Matsumoto, R. 1996, ApJ, 468, L37
Haerendel, G., Paschmann, G., Sckopke, N., Rosenbauer, H., Hedgecock P.C. 1978, J. Geophys. Res., 83, 3195
Hesse, M., Birn, J. 1993, J. Geophys. Res., 98, 3973

Kuijpers, J. 1995, in Coronal Magnetic Energy Releases, Proc. CESRA Workshop, Lecture Notes in Physics 444, Eds. A.O. Benz, A. Krüger, Springer Ver lag, Berlin, p. 135
Lockwood, M. 1991, J. Geophys. Res., 96, 5497
Matsumoto, R, Uchida, Y., Hirose, S. et al., 1996, ApJ, 461, 115
Nishida, A. 1989, Geophys. Res. Lett., 16, 227
Otto, A. 1990, Comput. Phys. Commun., 59, 185
Otto, A., Birk, G.T. 1992, J. Geophys. Res., 97, 8391
Otto, A., Birk, G.T. 1993, Geophys Res. Lett., 20, 2833
Paschmann, G., Haerendel, G., Papamastorakis, I. et al., 1982, J. Geophys. Res., 87, 2159
Pringle, J.E., Rees, M.J. 1972, A&A, 21, 1
Rastätter, L., Schindler, K. 1996, Astrophys. Lett. & Comm., 34, 357
Rastätter, L., Voge, A., Schindler, K. 1994, Phys. Plasmas, 1, 3414
Shakura, N.I., Sunyaev, R.A. 1973, A&A, 24, 337
Shi, Y., Wu, C.C. Lee, L.C. 1991, J. Geophys. Res., 96, 17627
Torkelsson, U., Schramkowski, G.P. 1996, A&AR, 7, 55
Uchida, Y., Low, B.C. 1981, JA&A, 2, 405
Van Ballegooijen, A.A. 1994, Space Sci. Rev., 68, 299
Ventura, J., Pines, D. 1991, Neutron Stars: Theory and Observation, NATO ASI-Series C 344, Kluwer, Dordrecht
Wang, Y.M, Robertson, J.A. 1984, A&A, 139, 93

This article was processed by the author using Springer-Verlag LaTeX A&A style file *L-AA* version 3.